PHYSICAL REVIEW E VOLUME 57, NUMBER 1 JANUARY 1998

Time resolved optical emission spectroscopy of an inductively coupled plasma in argon and oxygen

Masahiro Tadokoro, Hajime Hirata, Nobuhiko Nakano, Zoran Lj. Petrović,* and Toshiaki Makabe
Department of Electrical Engineering, Faculty of Science and Technology, Keio University, Yokohama 223, Japan
(Received 27 June 1997; revised manuscript received 22 September 1997)

We present the space-time resolved excitation data for a single coil inductively coupled plasma (ICP) reactor operating in collision dominated regime in argon and oxygen at 13.56 MHz. Robot assisted scanning was used in order to obtain Abel inverted radial profiles of emission and subsequently of the net excitation rate as well as the number density of excited states. The net excitation rate in argon has modulation close to the walls due to the azimuthal field time dependence and a large bulk value independent of the time presumably due to low energy electron-metastable atom collisions. The time resolved profile in oxygen shows a much more pronounced modulation due to the azimuthal field and a much lower degree of excitation for the center of the tube. At low pressures a structure is observed in the temporal dependence of the net excitation rate that is consistent with two different mechanisms of electron acceleration with phase shift of $\pi/4$: (I) by azimuthal field and (II) due to the drift motion in crossed electric and magnetic fields that leads to a motion in the azimuthal or radial direction and consequently to energy gain. [S1063-651X(98)50201-2]

PACS number(s): 52.70.Gw, 52.70.Kz, 52.25.Rv, 52.25.Sw

It is 50 years since the invention of the point-contact transistor [1]. During these 50 years, the progress and the system integration of semiconductor devices have been tremendous. Inductively coupled plasmas [2] (ICP) are one of the candidates for ULSI (ultra-large-scale integrated) microelectronic device fabrications in the next generation of the plasma as very reliable, high density sources that produce uniform treatment over large areas. The basic mechanisms of excitation in ICP have been studied by numerous theoretical [3–5] and experimental [6–11] procedures. It seems to have been established that in ICP the induced azimuthal electric field E_θ gives to electrons the energy that is required to sustain the discharge [12]. The temporal profile of the field may be associated with the temporal profile of the current in the coils while the radial profile is determined mostly by the skin depth of the plasma, i.e., the induced field is shielded by the plasma.

In this paper, we make an experimental prediction that there is an additional mechanism operating in ICP that may provide energy to electrons. The new mechanism is caused by the $\mathbf{E}\times\mathbf{B}$ drift motion under the radial static field $\mathbf{E}_r$ and the time varying axial magnetic field $\mathbf{B}_z(t)$, which will result in an electron acceleration in the azimuthal direction, $\{\mathbf{E}_r \times\mathbf{B}_z(t)\}\cdot\mathbf{E}_\theta$. It is physically equivalent to the energy gain in the radial direction by $-\{\mathbf{E}_\theta\times\mathbf{B}_z(t)\}\cdot\mathbf{E}_r$, and indistinguishable from it. The new mechanism will result in a different space-time dependence of the emission with a phase difference of $\pi/4$, as compared to the excitation due to the basic mechanism of electron acceleration purely by the azimuthal field [12].

The spatially resolved–time averaged experimental studies have contributed greatly towards understanding of some of the basic mechanisms of excitation kinetics, namely, to prove the importance of stepwise excitation [13,14], to show the azimuthal anisotropy of excitation through application of computer assisted tomography [15] and to indicate the spatial dependence of excitation (radical production) as a function of operating parameters such as power, pressure, and gas composition. Yet this technique cannot provide us with the results required to prove the proposed mechanism for energy coupling into ICP, so we had to use the much more difficult time resolved spectroscopy.

In this paper we apply time resolved spectroscopy to ICP in argon and in oxygen operating at low pressures (in a collision dominated regime). We are not aware of any other experimental studies of the time resolved spectra of low-pressure nonequilibrium ICP operating under conditions required for plasma processing applications. The basic experiment and procedure are the same as used before in our studies of ICP [13–15]. The ICP is produced in a quartz cylinder 10 cm in diameter and 20 cm in height. It is maintained by a single turn current coil with a waveform of $I_o\sin\omega t$, attached closely to the quartz tube on the outside and supplied by 13.56 MHz rf power through a matching box. A gas flow of 100 sccm of pure argon or oxygen is maintained by a system of leak valves and pumps used to evacuate the system. Power to the ICP including the matching network is measured by an in-line wattmeter. Peak-to-peak values of the radiofrequency (rf) voltage to the coil, V_{p-p} and currents close to the powered and the grounded terminals I_{p-p} are measured by a voltage probe connected between the coil and the matching box, and a pair of calibrated current probes. The effective dissipated power to the ICP is estimated by the current measurement of the coil in the reactor with and without plasmas under a same input power at the in-line wattmeter [16].

Optical emission profiles are obtained with the aid of an industrial four axis robot that can be controlled by computer to scan very accurately along a number of positions and directions. The optical detector is developed to have a detection efficiency independent of the position along the entire

*Also at Institute of Physics, University of Belgrade, P.O. Box 57, 11001 Belgrade, Yugoslavia.

path of the line of sight through the plasma, and it consists of a set of slits, a lens, and an optical fiber. The wavelength was selected by a monochromator and the light was detected by a photomultiplier. The system operates in a photon counting regime and it was absolutely calibrated by using a xenon arc lamp [15,17].

The important modification in the present work is that the photon counting system is now connected to a time-to-pulse height converter that is connected to a very fast multichannel analyzer, thus enabling a time resolved detection of emission. The triggering of the system is at the zero point crossing of the coil current from the calibrated current probe, and the system is reset when the photon is detected. The procedure to obtain and analyze the time resolved spectra is the same as used before in our studies of capacitively coupled plasmas (CCP) [17–19].

In our previous studies of computer aided tomography, we have employed both Abel inversion technique to an axially symmetric system [13,14] and Radon inversion to investigate the azimuthal asymmetry in the system [15]. Application of the radon inversion is forbiddingly difficult for obtaining the time resolved data; even the temporally averaged data requires many hours of scanning in different directions. Thus we have used the Abel inversion technique for time resolved data obtained over 16 h of signal averaging by scanning along the axis perpendicular to that of the input terminals, i.e., the axis that so far has given apparently symmetric profiles [15]. All measurements were performed at $z=$ 5 mm from the coil in the axial direction.

Scanning of 419.8 nm line of Ar I provides information on the short lived excited state Ar($3p_5$) with a radiative lifetime of 90 ns and with an excitation threshold of 14.57 eV. The effective lifetime is, however, reduced by collisions to as low as 70 ns at the highest pressure covered in this paper (i.e., 300 mTorr). The oxygen atom 844.6 nm line provides information on the density of the excited $3p^3P$ state with an excitation threshold of 10.98 eV. The natural lifetime of the upper state of the transition is 34 ns with a small reduction to around 30 ns at the highest pressure [20].

The absolute number densities of the excited states and the net excitation rates are obtained as a function of time and radial position from the deconvolution procedure of the measured spatiotemporal emission characteristics by using the available data for excited state quenching [17,20]. In Figs. 1 and 2 we show the data for the spatially and temporally resolved net excitation rates in argon at 400 W and in oxygen at 100 W in a wattmeter, respectively. The effective power dissipated to the ICP is estimated as 325 W, 330 W, and 340 W for 15 mTorr, 100 mTorr, and 300 mTorr in Ar, and 65 W and 70 W for 15 mTorr and 100 mTorr in O_2 by using the method mentioned above [16]. The data for argon show a degree of temporal modulation close to the wall that disappears with increasing pressure, while the radial profile peaking close to the wall becomes more pronounced. The obtained net excitation rate close to the axis of the discharge shows a statistically large scatter, which is a fundamental characteristic of the Abel inversion technique [21]. The data close to the walls are obtained from the signal collected over the entire space. Thus one should regard modulations that occur below $r=25$ mm as statistically insignificant though some systematic trends may persist even in that region.

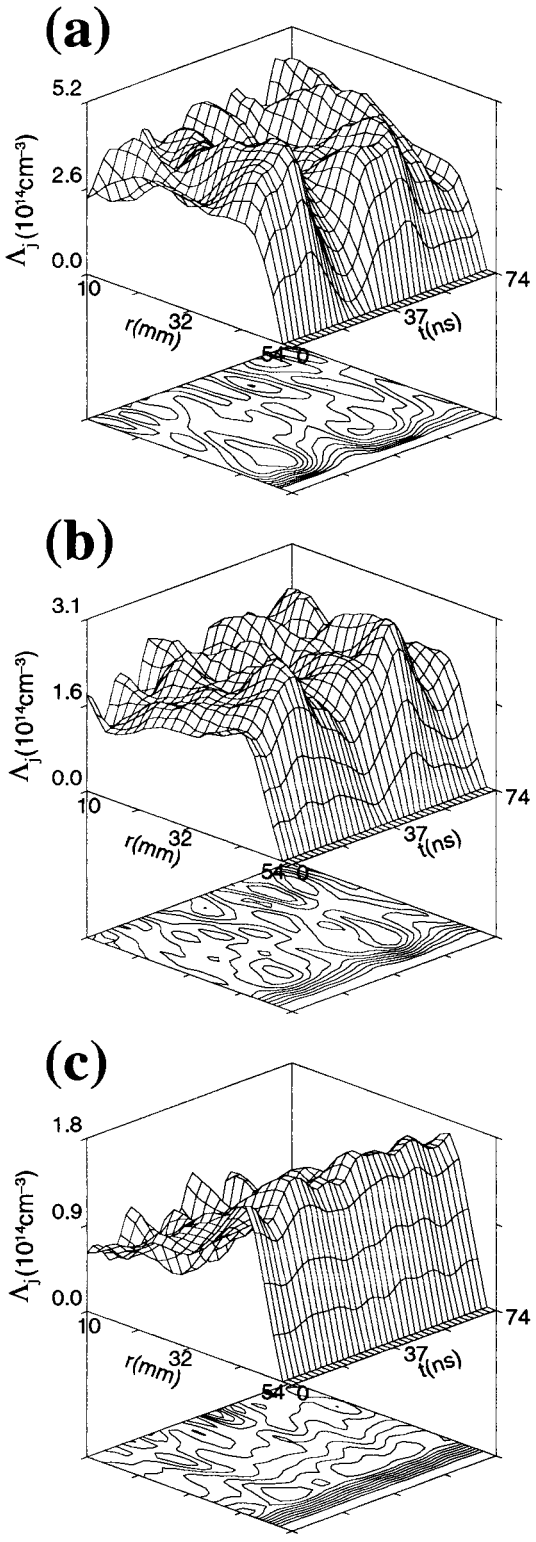

FIG. 1. Space-time resolved net excitation rate for excited state Ar($3p_5$) (400 W, 100 sccm). (a) 15 mTorr, (b) 100 mTorr, (c) 300 mTorr.

Therefore, the data less than $r<10$ mm are deliberately removed in Figs. 1 and 2. Extending measurements to more than 16 h of continuously running discharge was impractical because the properties of the system may change due to the long term changes in the environment temperature. We are,

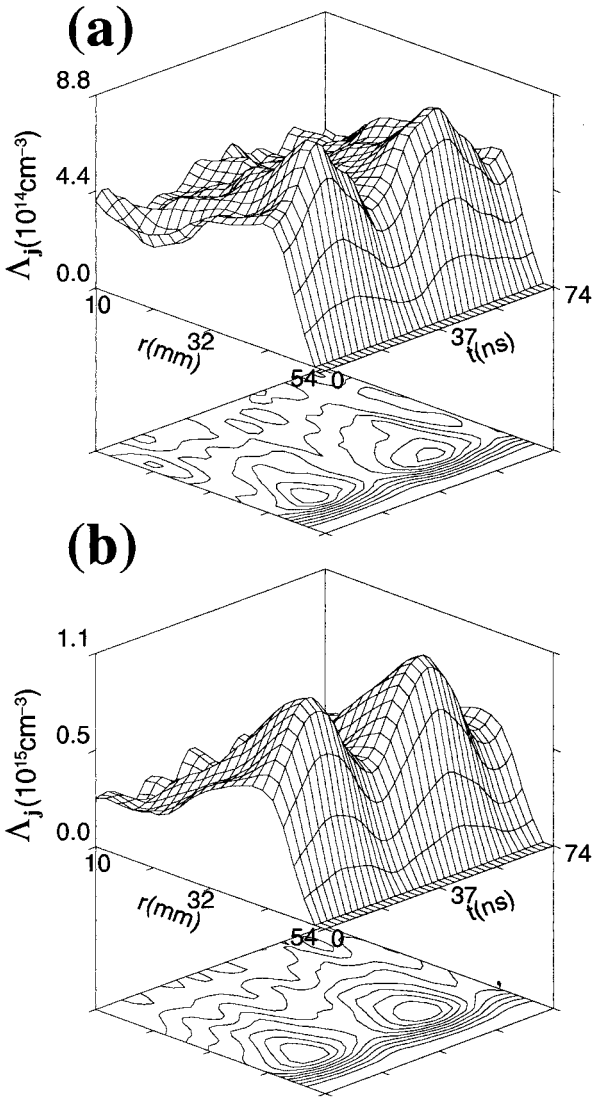

FIG. 2. Space-time resolved net excitation rate for excited state O($3p\ ^3P$) (100 W, 100 sccm). (a) 15 mTorr, (b) 100 mTorr.

however, satisfied that no such effects were significant over the period of measurements used in the present paper.

The data for oxygen shown in Fig. 2 were obtained at pressures of 15 mTorr and 100 mTorr. Measurements could be performed even at low powers of 100 W with still satisfactory statistics. The general characteristic of the results in oxygen is a much greater degree of modulation, which is consistent with our previous conclusions [13,14] that the radial profile of emission in argon is determined by electron-metastable collisions. In oxygen, however, the level of excitation close to the z axis is much lower than in argon (as compared to the peak value) and the modulations due to the time varying fields are much larger. In addition statistics is better, even at lower powers, to recognize the characteristics of temporal profiles.

A general characteristic of most profiles is the asymmetry of the temporal modulation of the net excitation rate. The more unexpected feature of the modulation is that the rising edge of the profile is more gradual, often showing some structure, while the trailing edge is much sharper. At 15

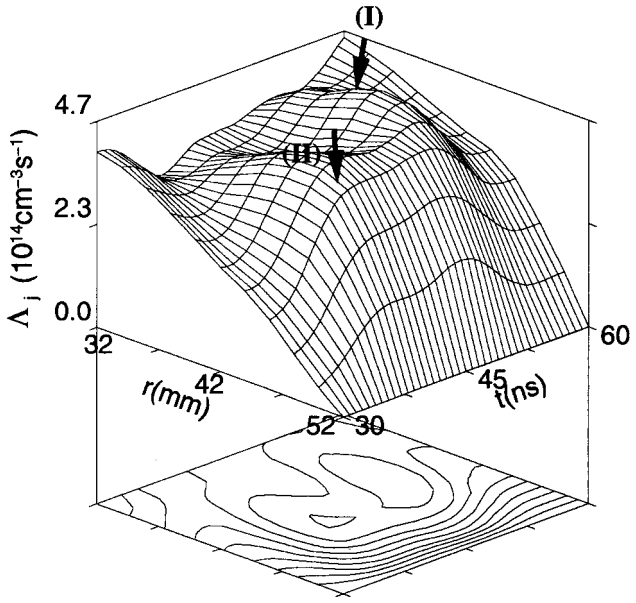

FIG. 3. A section of the space-time resolved net excitation rate for excited state Ar($3p_5$) (400 W, 100 sccm; 15 mTorr). The part marked by (I) shows the excitation due to electrons gaining energy from the azimuthal field, the region marked by (II) shows the contribution of the electrons that are accelerated by the $\mathbf{E}\times\mathbf{B}$ drift.

mTorr and 100 mTorr in Ar [Figs. 1(a) and 1(b)] two peaks are clearly observed during each half-period in temporal profiles at fixed radius, very close to the wall. This can be observed much better in Fig. 3, which shows an enlarged section of the spatiotemporal profile from Fig. 1(a) at 15 mTorr. The two ridges can be seen easily, the first one (I) extends deeper into the plasma and makes a larger overall contribution. The second ridge (II) occurs at an earlier time, $\pi/4$ of the period, ahead of the first (I) and it is located closer to the coil. It is difficult to distinguish the two peaks at higher pressure in Ar, since the net production rate has a strong dc component very close to the glass wall [see Fig. 1(c)]. We briefly discuss the two different excitation mechanisms. The first mechanism, shown in (I) in Fig. 3, is due to the acceleration of electrons purely in the azimuthal electric field. That is, the power deposition by electrons $P_\theta(t;\mathrm{I})$ shows the time dependence corresponding to the azimuthal electric field $E_\theta(t)$,

$$P_\theta(t;\mathrm{I}) = -en_e(r)V_{d\theta}(t,r)E_\theta(t,r) \propto E_\theta(t,r)^2 \propto \frac{1+\cos(2\omega t)}{2}, \tag{1}$$

where e is the electron charge, and n_e and $V_{d\theta}$ are the number density and the azimuthal drift velocity of electrons. The other mechanism occurs closer to the chamber walls and is associated with the static radial potential distribution base on an ambipolar wall sheath [see (II) in Fig. 3]. The ambipolar field, caused by the radial potential decrease close to the walls E_r gives rise to the directed motion of electrons. The time dependent magnetic field $B_z(t)$ gives rise to an additional drift of electrons in the azimuthal direction due to the

$\mathbf{E}_r \times \mathbf{B}_z(t)$ force. The drift in the azimuthal direction leads to an energy gain from the azimuthal field, which is time modulated as

$$P_\theta(t;\mathrm{II}) = -en_e(r)V_{d\mathbf{E}_r\times\mathbf{B}_z}(t,r)E_\theta(r,t) \propto B_z(t)E_\theta(t) \propto -\sin(2\omega t). \quad (2)$$

Here, $V_{d\mathbf{E}_r\times\mathbf{B}_z}(t,r)$ is the $\mathbf{E}_r\times\mathbf{B}_z$ drift velocity of electrons. That is, the first mechanism has a temporal dependence proportional to $\cos(2\omega t)$, while the second process is proportional to $-\sin(2\omega t)$. These temporal difference in modulation gives a phase difference of $\pi/4$ between the two excitation mechanisms. Note that, in the latter phase, when the azimuthal field changes sign, the drift changes direction, whereby electrons begin to loose their energy to the azimuthal field. It should be also noted in the second excitation mechanism that the mathematical relation $\{\mathbf{E}_r\times\mathbf{B}_z(t)\}\cdot\mathbf{E}_\theta(t) = -\{\mathbf{E}_\theta(t)\times\mathbf{B}_z(t)\}\cdot\mathbf{E}_r$ means the presence of the electron acceleration both in the azimuthal and the radial directions based on the $\mathbf{E}\times\mathbf{B}$ drift. They are physically indistinguishable from each other. In the case of O_2, the second peak in the net production rate is not detected. It may result from the lower electron density as compared with positive ions and from the reduction of the radial static electric field due to the presence of negative ions in O_2. Consequently, the second heating mechanism of electrons will be reduced in negative ion plasma in O_2.

In this paper we present the first, time resolved spectra of ICP obtained for nonequilibrium conditions used in plasma processing. Argon discharges are of interest for plasma etching, while oxygen discharges are of interest for plasma ashing, which is usually performed at somewhat higher pressures. Thus the pressure and power dependence of the results is of interest in designing the processes. It appears that in oxygen a much stronger time modulation as well as the radial dependence exists, making it more difficult to achieve uniform processing over large areas at higher pressures. The time modulation of the net excitation rate has a structure consistent with the two distinct space and time dependent processes of providing energy to electrons. The first is the main mechanism and the acceleration of electrons in the azimuthal electric field. The second is the electron heating due to the $\mathbf{E}\times\mathbf{B}$ drift. The latter peak leads the former by $\pi/4$. Two factors work to reduce the effect of the $\mathbf{E}\times\mathbf{B}$ acceleration mechanism at higher pressures. The first is that the static radial field E_r is smaller as the pressure increases [14] and the second is that the collisions will reduce the width of the region, where interaction can occur, so that the overlap of the three factors magnetic field profile, radial field profile, and azimuthal field profile may be reduced. The low magnetic field by a current coil in ICP has no influence on the transport of massive ions in plasmas.

No consideration of the $\mathbf{E}\times\mathbf{B}$ drift of electrons in ICP has been given in the previous modeling, to our knowledge, except for ours [22]. Further modeling for the specific geometry and other conditions in our system could, however, provide a valid test of the models both for argon and oxygen.

This work was supported in part by the Monbusho International Scientific Program, No. 08044169, and by the Keio University Special Grant-in-Aid for Innovative and Collaborative Research Project.

[1] J. Bardeen and W. H. Brattain, Phys. Rev. **74**, 230 (1948); B. Deal and J. Talbot, Interface (USA) **6**, 18 (1997).
[2] J. Hopwood, Plasma Sources Sci. Technol. **1**, 109 (1992).
[3] P. L. G. Ventzek, R. J. Hoekstra, and M. J. Kushner, J. Vac. Sci. Technol. B **12**, 461 (1994).
[4] A. P. Paranjpe, J. Vac. Sci. Technol. A **12**, 1221 (1994).
[5] U. Kortshagen and L. D. Tsendin, Appl. Phys. Lett. **65**, 1355 (1994).
[6] J. Hopwood, C. R. Guarnieri, S. J. Whitehair, and J. J. Cuomo, J. Vac. Sci. Technol. A **11**, 152 (1993).
[7] L. J. Mahoney, A. E. Wendt, E. Barrios, C. J. Richards, and J. L. Shohet, J. Appl. Phys. **76**, 2041 (1994).
[8] J. R. Woodworth, M. E. Riley, D. C. Meister, B. P. Aragon, M. S. Lee, and H. H. Sawin, J. Appl. Phys. **80**, 1304 (1996).
[9] U. Kortshagen, N. D. Gibson, and J. J. Lawler, J. Phys. D **29**, 1224 (1996).
[10] G. Mumken and U. Kortshagen, J. Appl. Phys. **80**, 6639 (1996).
[11] E. C. Benck, A. Schwabedissen, A. Gates, and J. R. Roberts, J. Vac. Sci. Technol. A (to be published).
[12] V. Vahedi, M. A. Lieberman, G. DiPeso, T. D. Rognlien, and D. Hewett, J. Appl. Phys. **78**, 1446 (1995).
[13] A. Okigawa, T. Makabe, T. Shibagaki, N. Nakano, Z. L. Petrović, T. Kogawa, and A. Itoh, Jpn. J. Appl. Phys. **35**, 1890 (1996).
[14] A. Okigawa, Z. Lj. Petrović, M. Tadokoro, T. Makabe, N. Nakano, and A. Itoh, Appl. Phys. Lett. **69**, 2644 (1996).
[15] A. Okigawa, M. Tadokoro, A. Itoh, N. Nakano, Z. Lj. Petrović, and T. Makabe, Jpn. J. Appl. Phys. **36B**, 4605 (1997).
[16] P. A. Miller, G. A. Hebner, K. E. Greenberg, P. D. Pochan, and B. P. Aragon, J. Res. Natl. Inst. Stand. Technol. **100**, 427 (1995).
[17] F. Tochikubo, T. Kokubo, S. Kakuta, A. Suzuki, and T. Makabe, J. Phys. D **23**, 1184 (1990).
[18] F. Tochikubo, Z. Lj. Petrović, S. Kakuta, N. Nakano, and T. Makabe, Jpn. J. Appl. Phys. **33**, 4271 (1994).
[19] Z. Lj. Petrović, F. Tochikubo, S. Kakuta, and T. Makabe, J. Appl. Phys. **73**, 2163 (1993).
[20] J. Bittner, K. kohse-Hoinghaus, U. Meier, and Th. Just, Chem. Phys. Lett. **143**, 571 (1988).
[21] T. Kitajima, M. Izawa, N. Nakano, and T. Makabe, J. Phys. D **30**, 1783 (1997).
[22] K. Kondo, H. Kuroda, and T. Makabe, Appl. Phys. Lett. **65**, 31 (1994).